



RESEARCH ARTICLE

# A modeling radiocarbon dating for the founding of Yan Vassal State in Western Zhou Dynasty

Xinyi Ouyang<sup>1</sup> , Xiaohong Wu<sup>1</sup> , Jing Wang<sup>2</sup>, Yan Pan<sup>1</sup>, YiHsien Lin<sup>1</sup>, Jianing He<sup>1</sup>, Jingning Guo<sup>2</sup> and Jianfeng Cui<sup>1</sup>

<sup>1</sup>Key Laboratory of Archaeological Science (Ministry of Education), School of Archaeology and Museology, Peking University, Beijing 100871, China and <sup>2</sup>Beijing Institute of Archaeology, Beijing 10009, China

**Corresponding authors:** Xiaohong Wu; Email: [wuxh@pku.edu.cn](mailto:wuxh@pku.edu.cn), Jingning Guo; Email: [bjkaogubaogao@163.com](mailto:bjkaogubaogao@163.com)

**Received:** 10 March 2024; **Revised:** 25 September 2024; **Accepted:** 22 October 2024

**Keywords:** AMS radiocarbon dating; Liulihe Site; Vassal State of Yan; Bronze Age; wiggle-match

## Abstract

Western Zhou Dynasty (ca. 1046–771 BC) was established soon after conquering the Shang Dynasty (ca. 1600–1046 BC) and brought about the earliest enfeoffment system in Chinese history. Yan was one of the vassal states of the same clan as Zhou. According to historical records, the capital of Yan state was located near Yan mountain, which is now known as the Liulihe site in the Fangshan District, Beijing. This study carries out the high-precision dating of two newly discovered Western Zhou Dynasty noble tombs at the Liulihe site. The man in tomb M1902 participated in the groundbreaking ceremony of Yan's capital according to inscriptions on the bronze vessel found in this tomb. Samples of different materials, especially different parts of human skeletons from the tombs, were selected to form a sample series in chronological order. Wiggle-matching models were established in OxCal program based on the growth and development time of different teeth and bones of human skeletons. More accurate ages were acquired for the death of the individuals. The results indicate that the most probable distribution range of the death date of the individual in M1902 is about 1045–1010 BC. The radiocarbon dates of M1902 give important chronological information about the founding of Yan state, and they are very close to those of the year in which King Wu of Zhou conquered the Shang Dynasty.

## Introduction

Establishing a high-precision radiocarbon-based chronology of early Dynastic China is important not only for understanding Chinese early history, but also for examining the contradiction between the broad uncertainty of single calibrated radiocarbon dates and the fine chronology of historical records. The newly discovered noble tombs at Liulihe (琉璃河) site in Beijing, where the capital of Yan (燕) state was located during the Western Zhou (西周) Dynasty, provided very important materials for these studies.

The enfeoffment of Yan state occurred in the early Western Zhou Dynasty. The beginning of the Western Zhou Dynasty is approximately dated to 1046 BC (Xia-Shang-Zhou Chronology Project 2022). Yan's enfeoffment occurred slightly later than this date. Chinese historical records, specifically the *Shiji* (史记), document in its section “Duke Shao's Aristocratic Family of Yan” (燕召公世家) that “King Wu (武) of Zhou defeated Shang, and enfeoffed Shao (召) in Northern Yan.” Duke Shao, the son of King Wen (文), assisted King Wu in establishing the Zhou Dynasty. Yan State is located in the region of Yan Mountain at a crucial crossroad from the Central Plains to the northeast and the Mongolian grasslands (Figure 1), as the agricultural and pastoral transitional zone in northern China, with complex and diverse climatic and cultural conditions. Its territory held a very important strategic position.

Although the exact location of the Yan Vassal state's capital was not documented in literature, a substantial site with abundant remains from Western Zhou Dynasties was found in Dongjialin (董家林)



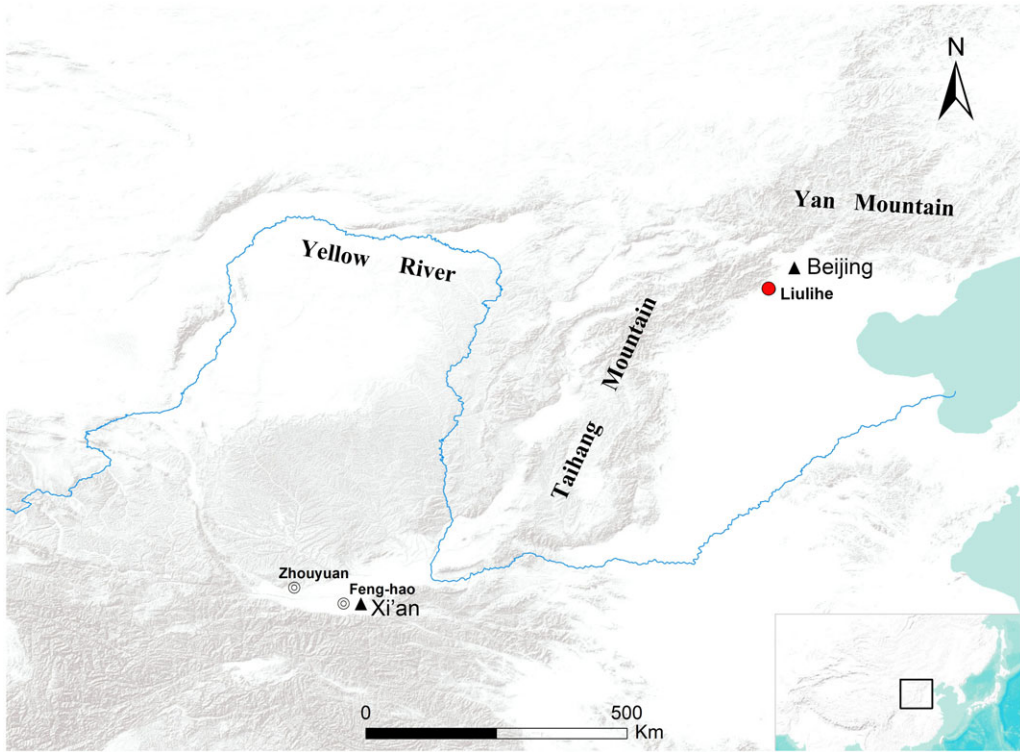


**Figure 1.** Location of Liulihe site. Zhouyuan site and the Feng-Hao site are capitals of the Western Zhou dynasty. The triangle legend presents key modern cities.

and Huangtupo (黄土坡) villages at Liulihe Town in Fangshan District, Beijing, named Liulihe site. Extensive excavations at Liulihe site have been conducted since the latter half of the 20th century (Beijing Cultural Relics Team 1963; Department of Archaeology PKU and Institute of Archaeology of Beijing 1996; Institute of Archaeology CASS et al. 1974; Institute of Archaeology CASS and Institute of Archaeology of Beijing 1984; 1990; Institute of Archaeology of Beijing 1995; Institute of Archaeology of Beijing and Department of Archaeology PKU 1996; Liulihe Archaeology Team 1997; Institute of Archaeology of Beijing et al. 2000; Lou 2002). The various functional zones were revealed in a total area of approximately 5.25 square kilometers, including residential areas with remains of large buildings and burial areas. Over 400 tombs have been excavated, with many chariot pits, sacrificial pits and valuable artifacts discovered. The important discoveries at Liulihe site are the precious bronze ritual vessels of the early Western Zhou Dynasty, such as the Yan Hou Jin Ding (匱侯堇鼎), Tai Bao Ke He (太保克盃), and Bo Ju Li (伯矩鬲) (Figure 2). These valuable bronze artifacts were inscribed with the characters of the names of the important historical personages as “Yan Hou 匱侯,” “Bo Ju 伯矩,” and “Tai Bao Ke 太保克.” Ke is the first-born son of Duke Shao. When Duke Shao was enfeoffed in the vassal state of Yan, he continued to stay by the side of King of Zhou to assist in governance, and sent his son, Ke, to replace him in governing the vassal state of Yan.

A new round excavation of Liulihe site has been carried out since 2019, leading to the discovery of two noble burials with bronze vessels bearing inscriptions about the founding event of the Yan state. These discoveries, together with the historical records, provide important evidences for the Liulihe site as the location of the initial capital of Yan State in the early Western Zhou Dynasty. It is a breakthrough in the field of Bronze Age studies in China and the discoveries may also serve as a crucial role for investigating the history of urbanization of Beijing.



**Figure 2.** Bronze ritual vessels and their inscriptions found at Liulihe site. From top to bottom are Yan Hou Jin Ding (偃侯墓鼎), Tai Bao Ke He (太保克盃), and Bo Ju Li (伯矩鬲). Pictures cited from Wu (2012).

Obtaining high-precision ages of Liulihe site is essential for understanding the enfeoffment of the Yan state during the formation of the Western Zhou Dynasty in Zhou's northern territory, and also for understanding the urban history of Beijing. Radiocarbon dating has been extensively used in the

chronological research of early Dynastic China since the end of last century (Chen 2023; Lee 2002; Li et al. 2023; Liu et al. 2021; Xia-Shang-Zhou Chronology Project 2022). Notably, radiocarbon dating of burial M1193 at the Liulihe site in 1990s yielded important insights. This burial contains bronze vessels, specifically Jue (爵) and He (盃), that have the inscriptions about the foundation of the Yan Vassal state. The results of calibrated radiocarbon dates indicate that the date range in 68.3% probability is about 1032 BC to 911 BC, which can be considered as the upper limit of the burial's date (Xia-Shang-Zhou Chronology Project 2022; Zhang et al. 2003). Due to the presence of the plateau areas on the calibration curve, the range of radiocarbon dates expands after calibration. The time period of late Shang (商) Dynasty to early Western Zhou Dynasty is just right in this situation. It is difficult to get a fine radiocarbon chronology matching with the historical records from the single calibrated radiocarbon ages. The employing of Bayesian modeling has greatly refined the precision of calibrated dates (Bayliss 2009, 2015; Wood 2015). The prior conditions related to the radiocarbon dates used to design the Bayesian models mostly originate from the stratigraphic relationships caused by the site formation (Li et al. 2023), sometimes from the chronological orders according to the artifact typology (Xia-Shang-Zhou Chronology Project 2022). Investigations on chronological differences among different skeletal types within an individual have significantly impact on the radiocarbon dating research (Calcagnile et al. 2013; Geyh 2001; Hedges et al. 2007). Multiple tissues from a single individual were often analyzed by bomb pulse radiocarbon dating to better determine the year of birth and death in forensic science (Hodgins 2009; Johnstone-Belford et al. 2022; Ubelaker et al. 2006). Recent attempts have been made by using ancient samples, such as otic capsule-rib samples (Chmielewski et al. 2021) and dentine bulk samples (Dury et al. 2021; Millard et al. 2020). This paper applies the sampling strategy to the two newly discovered noble burials at Liulihe site and develops a Bayesian model for individual human skeletal assemblage consisting of dentine sequence, rib and limb bone samples in a relative chronological order by considering the inbuilt age of the samples, in an effort to get the fine radiocarbon-based chronology of early Western Zhou Dynasty. The attempt may serve as a good solution to determine the accurate high-precision dating problem in the Shang and Zhou dynasties in a manner consistent with the historical records.

## Materials and methods

### *Sample selection*

In order to get the high-precision results, we established dating sequences based on the temporal differences of radiocarbon signals in different teeth and different types of individual skeletons.

For M1902, anthropological information suggests that the individual buried in the tomb was 40–45-year-old, likely male. The samples selected from the human skeleton include the first molar of left mandibular, the left humerus, and rib bones. Additionally, the coffin wood, plant woven materials attached to the bronze vessel, and sacrificial animals from this tomb were chosen. The results of radiocarbon dating obtained from the plant and animal samples, as well as the time information from the inscriptions on the bronze vessels, will be used to assess the effectiveness of dating results obtained from the individual's osteological assemblage.

Regarding M1905, the available dating samples are restricted, as there are no sacrificial animal bones or plant remains. Only human skeleton existed that are highly suitable for dating purposes. The samples selected for radiocarbon dating in M1905 include the right maxillary first molar, the left tibia, and rib bones of the individual, who has been identified as a male between the ages of 40 and 45.

### *Sample Preparation and Analysis*

All sample preparation were conducted at Radiocarbon Dating Laboratory, School of Archaeology and Museology, Peking University.

Incremental samples were obtained from the mandibular or maxillary first molars (M1) of the individuals. The tooth surfaces were cleaned and then embedded in high-strength gypsum-forming material. Using the METCUT-5 low-speed metallographic cutting machine from MetLab, each tooth was longitudinally sectioned into three pieces. One portion was selected for radiocarbon dating, while the remaining two were preserved for subsequent analysis.

The tooth slices were pretreated followed methods developed by Beaumont (Beaumont et al. 2013) and Czermak (Czermak et al. 2018, 2020). The tooth sections were demineralized in a 0.5M hydrochloric acid solution at room temperature for one week. After demineralization, the tooth sections were horizontally divided into approximate thirds using a sterile surgical blade, with specific anatomical locations determined with reference to tooth development stages (AlQahtani et al. 2010). These sequential samples were numbered from the crown to the root as 1–3. Subsequently, each subsample underwent treatment with 1% NaOH solution followed by 0.5M hydrochloric acid, with thorough rinsing using deionized water among steps. The tooth samples were then hydrolyzed in an HCl solution with pH 2–3 at 90°C for 20 hours, followed by centrifugation to collect the supernatant. After freeze-drying, collagen was obtained.

The percentage contents and atomic weight ratio of carbon and nitrogen in collagen samples were measured using Elementar's vario PYRO cube element analyzer. Radiocarbon dating was measured at the AMS Center, School of Physics, Peking University.

### *Calibration and Bayesian modeling*

Radiocarbon measurements were calibrated using OxCal v4.4.4 program (Bronk Ramsey 2009, 2021) with the IntCal20 calibration curve (Reimer et al. 2020). We employed the Sequence model based on the “osteological sequence” of an individual. Three sequential samples derived from either the upper or lower first molar (M1), considered as three independent events, were included within the temporal framework. Both single and multiple types of bone samples were also classified as independent events. To construct a coherent temporal framework, we systematically assigned intervals between these independent events, informed by the osteological characteristics inherent to each sample. The age intervals established between these sequential events are approximations, accompanied by a degree of uncertainty. The uncertainty is quantitatively modeled to follow a normal distribution, enabling us to incorporate and address the inherent variability and unpredictability associated with archaeological and osteological information.

The determination of age intervals for dentine sequential samples was based on the precise timing of tooth formation and development (AlQahtani et al. 2010). Both tooth samples were M1 and the formation time of M1 spends approximately 10 years. Therefore, the time interval between each sequential sample of the tooth as one third of the whole tooth was set to 3.3 years. The tooth samples “-1” to “-3” represented time information of the individual at about 1.7, 5, and 8.3 years of age, respectively, with a 6.6-year gap between the earliest and latest samples. A margin of error of  $\pm 3.3$  years was applied in the analysis.

Determining age intervals between different types of bone samples is a more complex process. Typically, limb bones provide an indication of an individual's radiocarbon levels throughout their early years, whereas other bone types like ribs and vertebrae show more recent radiocarbon signals that are closer to the moment of death (Fahy et al. 2017; Geyh 2001; Hedges et al. 2007). The specific span of these age intervals is closely related to the age at death of the individual. Referring to previous experiments on modern samples (Geyh 2001; Johnstone-Belford et al. 2022; Ubelaker et al. 2015, 2022) and modeling studies (Barta and Štolc 2007; Hedges et al. 2007), age intervals between final molar samples, long bones, and rib bone samples were set at 15 years and 10 years, respectively, for the two male individuals who both died at the age of 40–45.

The Date function was used to estimate the time of individual's death, with the required parameter (offset) as that the individual's age at death minus the representative age of the skeletal sample closest to

the time of death. The Date function gives the highest posterior density (hpd) range for the date of an event that is not directly dated but is related to previous occurrences through the prior in the model, and visualizes them. This function, as explained in the OxCal manual with a wiggle-match example of tree-ring samples ([https://c14.arch.ox.ac.uk/oxcalhelp/hlp\\_analysis\\_eg.html#wiggle](https://c14.arch.ox.ac.uk/oxcalhelp/hlp_analysis_eg.html#wiggle)), finds application in dating paleoenvironmental sediment cores (Staff et al. 2011) and archaeological contexts (Dury et al. 2021).

## Results

The results of the radiocarbon dating are presented in Table 1. With the exception of one tooth slice sample (BA220744-1), which did not yield sufficient collagen for carbon and nitrogen elemental analysis, the quality indicators for all other collagen samples fall within an acceptable range. The yield of collagen is greater than 1%, the carbon content comprising 30–50% of the weight of the collagen, and the C:N atomic weight ratio within the range of 2.9–3.5 (van Klinken 1999).

The sequence models of M1902 and M1905 are shown in Figure 3 and Supplementary Material. Modeled calibrated dates and individual's death time from M1902 and M1905 are shown in Figure 4. The agreement factor of the model of M1902 is 68% and of the M1905 is 130%.

## Discussion

Based on the modeling (only including the human skeletal samples), the estimated death date of the individual in M1902 is between 1092 to 1010 BC with 68.3% probability and between 1100 to 998 BC with 95.4% probability. The death date of the individual in M1905 is between 1002 to 976 BC with 68.3% probability and between 1036 to 950 BC with 95.4% probability, which is slightly later than M1902.

To evaluate the Bayesian modeling results, further samples from M1902 were analyzed (Table 1; Figure 5).

Three plant samples (wood samples from coffin lid and board, plant weaving adhering to the inner wall of the mouth of a bronze vessel) were selected. The coffin lid wood was identified as pine (genus *Pinus* L.), but the board wood was unidentifiable. The wood samples had no preserved bark, making it challenging to distinguish between sapwood or heartwood. The woven material was identified as bamboo (subfamily *Bambusoideae*). Considering that the growth and felling of wood and bamboo occurred before the time of the burial event, it is anticipated that the chronological results for the three plant samples will precede the time of individual's death (specifically, the time of burial, considering the primary burial deposition). The pine wood used for the coffin lid showed the oldest age results, in line with the long lifespan of pine and its use in constructing large coffin lids. The age ranges for the board wood and bamboo weaving were later. All the dates of the plant samples are not later than the individual's death date (with a 95.4% probability), aligning with our anticipation.

Additionally, two sacrificial animal samples were tested: one is the dog found in the waist-pit located at the bottom of the tomb (specifically its humerus) and the other is the lamb found in the head chamber (its radius). Both were identified anatomically as being around one year old, and were placed in the tomb as part of the funeral ceremony. Therefore, their ages represented the date of the burial event, and should align with the calculated time of the human's death, as determined by modeling, as shown in Figure 5. By considering that the death events of these three entities occurred simultaneously, the main probability distribution of the burial date is 1045–1010 BC (Figure 5), which is in the time period of Early Western Zhou Dynasty.

The chronological result is remarkably consistent with the inscriptions on the bronze vessel from the tomb M1902 (Shi 2022), as below:

**Table 1.** A summary of dating samples reported in this study. The calibrated range showed here is unmodeled

Lab no.	Context	Individual	Sample type	Yield (%)	%C	%N	C:N	<sup>14</sup> C age ±1σ year BP	Calibrated range	Calibrated range
									68.3%	95.4%
BA220734	M1902	Human	Humerus	10.13	43.27	15.92	3.17	2845±20	1046BC (14.2%) 1028BC 1020BC (42.2%) 977BC 951BC (11.8%)	1106BC (1.5%) 1096BC 1082BC (2.1%) 1068BC 1056BC (91.8%) 924BC
BA220736-1	M1902	Human	M1	—	42.42	15.66	3.16	2950±20	1206BC (68.3%) 1125BC	1255BC (1.1%) 1248BC 1226BC (94.3%) 1054BC
BA220736-2	M1902	Human	M1	—	42.34	15.51	3.19	2905±20	1124BC (65.1%) 1047BC 1027BC (3.2%) 1021BC	1200BC (8.1%) 1170BC 1164BC (6.5%) 1142BC 1130BC (80.9%) 1012BC
BA220736-3	M1902	Human	M1	—	41.96	15.42	3.17	2890±20	1112BC (58.8%) 1046BC 1030BC (9.5%) 1020BC	1192BC (2.3%) 1176BC 1158BC (1.7%) 1146BC 1128BC (91.4%) 1004BC
BA220742	M1905	Human	Tibia	13.16	43.51	16.09	3.15	2800±25	986BC (68.3%) 916BC	1042BC (0.5%) 1036BC 1016BC (92.4%) 896BC 870BC (2.5%) 848BC
BA220743	M1905	Human	Rib	13.43	43.32	15.87	3.19	2815±25	1000BC (68.3%) 930BC	1046BC (3.5%) 1028BC 1020BC (92.0%) 902BC
BA220744-1	M1905	Human	M1	—	—	—	—	2890±25	1116BC (54.8%) 1042BC 1035BC (13.5%) 1016BC	1199BC (4.7%) 1171BC 1164BC (3.7%) 1142BC 1130BC (87.1%) 989BC

(Continued)

**Table 1.** (Continued)

Lab no.	Context	Individual	Sample type	Yield (%)	%C	%N	C:N	<sup>14</sup> C age ±1σ year BP	Calibrated range	Calibrated range
									68.3%	95.4%
BA220744-2	M1905	Human	M1	—	42.00	15.45	3.17	2875±25	1110BC (12.3%) 1090BC 1086BC (13.8%) 1064BC 1059BC (42.2%) 1009BC	1188BC (1.0%) 1178BC 1154BC (0.6%) 1148BC 1126BC (90.7%) 974BC 954BC (3.1%) 934BC
BA220744-3	M1905	Human	M1	—	41.63	15.48	3.14	2850±20	1048BC (62.5%) 980BC 948BC (5.8%) 939BC	1108BC (3.2%) 1092BC 1086BC (4.2%) 1066BC 1058BC (88.1%) 928BC
BA220746	M1902	Plant	Bamboo weaving	—	—	—	—	2890±20	1112BC (58.8%) 1046BC 1030BC (9.5%) 1020BC	1192BC (2.3%) 1176BC 1158BC (1.7%) 1146BC 1128BC (91.4%) 1004BC
BA220747	M1902	Plant	Coffin lid wood (pine)	—	—	—	—	3085±25	1408BC (26.2%) 1376BC 1350BC (42.0%) 1302BC	1419BC (95.4%) 1276BC
BA220748	M1902	Plant	Coffin board wood (unidentifiable)	—	—	—	—	2925±25	1196BC (13.4%) 1173BC 1162BC (11.9%) 1143BC 1130BC (43.0%) 1054BC	1215BC (92.8%) 1044BC 1031BC (2.7%) 1018BC
BA221832	M1902	Dog	Humerus	2.02	39.42	14.68	3.13	2840±25	1045BC (9.1%) 1031BC 1019BC (41.1%) 971BC 956BC (18.1%) 932BC	1108BC (2.0%) 1094BC 1084BC (2.6%) 1066BC 1058BC (90.9%) 917BC
BA221834	M1902	Sheep	Radius	10.52	42.36	15.68	3.15	2820±25	1006BC (68.3%) 930BC	1047BC (5.0%) 1027BC 1021BC (90.4%) 906BC



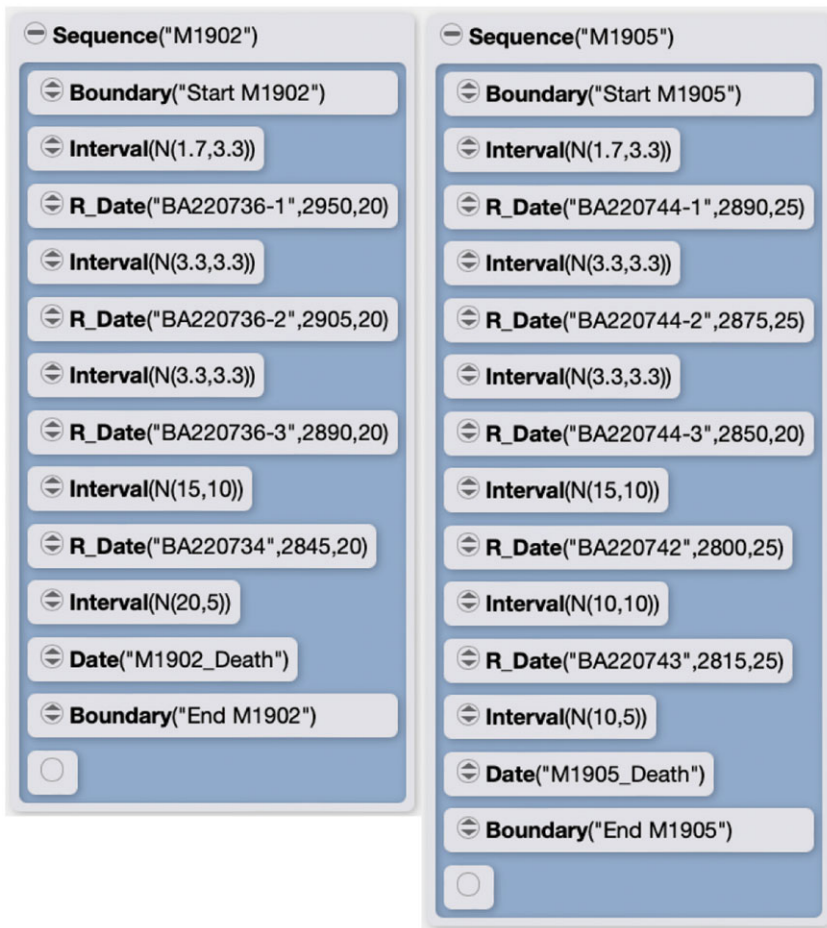


**Figure 3.** The Bayesian model for M1902 and M1905.

“Taibao (太保) built the Yan City and then held a ceremony in the palace of the Duke of Yan. Taibao rewarded the historiographer Huan (奂) with a quantity of shells, which were used in casting bronze vessels commemorating Father Xin (辛). In the year of Geng (庚).”

[“太保墉厦，延宛厦侯宫，太保赐作册奂贝，用作父辛宝尊彝。庚。”]

This inscription vividly records a significant historical event during the early Western Zhou period, marking the establishment of the Yan State. Huan, the owner of M1902, clearly possesses the expertise of a state historiographer. He participated in the ceremony celebrating the establishment of the city and was bestowed a reward by the esteemed official Duke Shao of the Western Zhou dynasty. Clearly, Huan, who was in his forties, deceased in close proximity to or shortly after the completion of Yan City. Therefore, the most probable distribution range of Huan’s death is 1045–1010 BC.

For M1905, the unmodeled calibrated date of the rib sample (BA220743) is 1000–930 BC (in 68.3% probability) and 1046–902 BC (in 95.4% probability), which were usually regarded as the burial’s date. After the calibration with our model, the death date of the individual in this tomb was narrowed down to the range of 1002–976 BC (in 68.3% probability) and 1036–950 BC (in 95.4% probability). The most probable distribution range of the death date of the individual in M1905 is 1015–950 BC (94.7%).

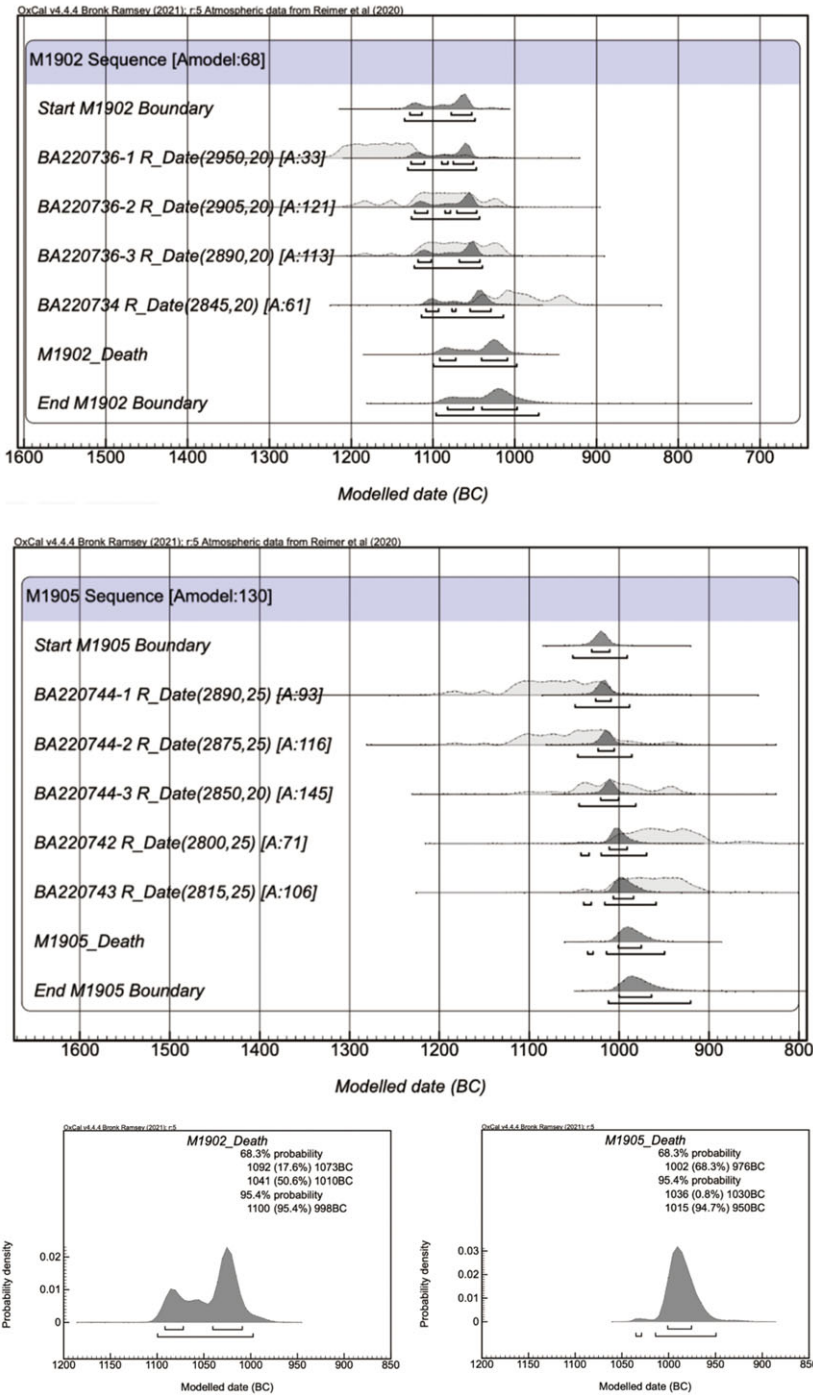


**Figure 4.** Sequence model of radiocarbon dates of the skeletons from M1902 and M1905, based on the osteological sequence. Unmodeled dates are plotted in light gray, while modeled calibrated dates are plotted in dark gray.

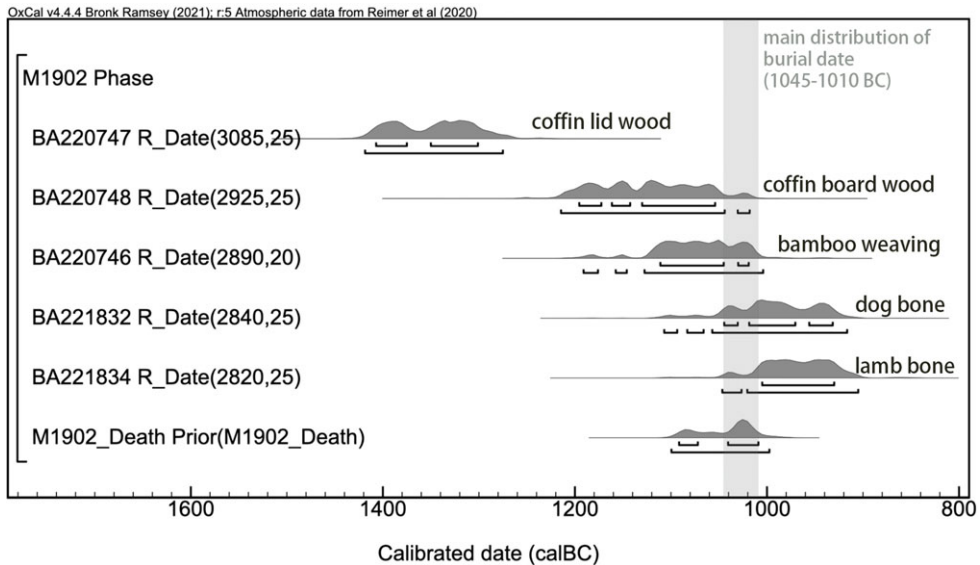


**Figure 5.** Additional calibrated dates (non-human tissue samples) from M1902. The “M1902\_Death” estimated in previous Sequence model was inserted here with the Prior command in OxCal.

## Conclusion

This study has utilized Bayesian modeling to establish a chronological sequence of the bone and tooth samples belonging to a single individual, thereby enhancing the accuracy of the time frame when the noble burials at the Liulihe site were performed. Crucially, the inscriptions on the bronze discovered in M1902 suggest that the individual buried in the tomb took part in the founding ceremony of the Yan city. Therefore, based on the estimated death date of man in M1902 (1045–1010 BC), we can then infer that the formation of the Yan state slightly predated the death of the individual in M1902. This case study highlights the importance of the temporal information provided by the samples themselves, even while refining the dating method and statistical analysis approaches. It not only clarifies the formation date of the Yan state through modeled radiocarbon dating but also demonstrates the application of osteological sequential sampling from single individual for high-precision radiocarbon dating in archaeological studies.

**Supplementary material.** To view supplementary material for this article, please visit <https://doi.org/10.1017/RDC.2024.117>

**Acknowledgments.** We acknowledge the field work and support of Liulihe archaeology team. We thank Yue Wang, Yihang Zhou, Renjie Ma, Kun Yang and Zhipeng Li for their assistance in document collection, preparation and species identification of samples, and discussion of Bayesian Models. We would also like to thank three anonymous reviewers and editors for their valuable feedback and help prior to publication. This work was supported by the Key project of National Social Science Foundation: “Chronological Study of Bronze Culture on the Silk Road”, 2017–2024, Project Number: 16ZDA144, and National Key Research and Development Program of China, Project Number: 2020YFC1521604.

## References

- AlQahtani SJ, Hector MP and Liversidge HM (2010) Brief communication: The London atlas of human tooth development and eruption. *American Journal of Physical Anthropology* **142**(3), 481–490.
- Barta P and Štolc S (2007) Hbco correction: Its impact on archaeological absolute dating. *Radiocarbon* **49**(2), 465–472.
- Bayliss A (2009) Rolling out revolution: Using radiocarbon dating in archaeology. *Radiocarbon* **51**(1), 123–147.
- Bayliss A (2015) Quality in bayesian chronological models in archaeology. *World Archaeology* **47**(4), 677–700.
- Beaumont J, Gledhill A, Lee-Thorp J and Montgomery J (2013) Childhood diet: A closer examination of the evidence from dental tissues using stable isotope analysis of incremental human dentine. *Archaeometry* **55**, 277.

- Beijing Cultural Relics Team (1963) 北京房山县考古调查简报 (A brief report on the archaeological survey of fangshan county, Beijing). *考古 (Kaogu)* **1963**.03, 115–121+129.
- Bronk Ramsey C (2009) Bayesian analysis of radiocarbon dates. *Radiocarbon* **51**(1), 337–360.
- Bronk Ramsey C (2021) Oxcal v4.4.4. Oxford: Oxford Radiocarbon Accelerator Unit.
- Calcnigne L, Quarta G, Cattaneo C and D'Elia M (2013) Determining  $^{14}\text{C}$  content in different human tissues: Implications for application of  $^{14}\text{C}$  bomb-spike dating in forensic medicine. *Radiocarbon* **55**(3), 1845–1849.
- Chen X (2023) Radiocarbon dating and its applications in Chinese archeology: An overview. *Frontiers in Earth Science* **11**.
- Chmielewski TJ, Hałaszkó A, Goslar T, Cheronet O, Hajdu T, Szeniczey T and Virag C (2021) Increase in  $^{14}\text{C}$  dating accuracy of prehistoric skeletal remains by optimised bone sampling: Chronometric studies on eneolithic burials from mikulin 9 (poland) and urziceni-vada ret (Romania). *Geochronometria* **47**(1), 196–208.
- Czermak A, Fernández-Crespo T, Ditchfield PW and Lee-Thorp JA (2020) A guide for an anatomically sensitive dentine microsampling and age-alignment approach for human teeth isotopic sequences. *American Journal of Physical Anthropology* **173**(4), 776–783.
- Czermak A, Schermelleh L and Lee-Thorp J (2018) Imaging-assisted time-resolved dentine sampling to track weaning histories. *International Journal of Osteoarchaeology* **28**(5), 535–541.
- Department of Archaeology PKU, Institute of Archaeology of Beijing (1996) 1995 年琉璃河周代居址发掘简报 (The 1995 season of excavation of the dwelling site of the Zhou Dynasty at Liulihe). *文物 (Wenwu)* **1996**.06, 4–15+97+12.
- Dury JPR, Lidén K, Harris AJT and Eriksson G (2021) Dental wiggle matching: Radiocarbon modelling of sub-sampled archaeological human dentine. *Quaternary International* **595**, 118–127.
- Fahy GE, Deter C, Pitfield R, Miszkiewicz JJ and Mahoney P (2017) Bone deep: Variation in stable isotope ratios and histomorphometric measurements of bone remodelling within adult humans. *Journal of Archaeological Science* **87**, 10–16.
- Geyh MA (2001) Bomb radiocarbon dating of animal tissues and hair. *Radiocarbon* **43**(2B), 723–730.
- Hedges REM, Clement JG, Thomas CDL and O'Connell TC (2007) Collagen turnover in the adult femoral mid-shaft: Modeled from anthropogenic radiocarbon tracer measurements. *American Journal of Physical Anthropology* **133**(2), 808–816.
- Hodgins GW (2009) Measuring atomic bomb-derived  $^{14}\text{C}$  levels in human remains to determine year of birth and/or year of death. NIJ Report.
- Institute of Archaeology CASS, Beijing Cultural Relics Management Office, Fangshan County Bureau of Culture and Education, Liulihe Archaeology Team (1974) 北京附近发现的西周奴隶殉葬墓 (Western Zhou slave martyrdom tomb discovered near Beijing). *考古 (Kaogu)* **1974**.05, 309–321+344–348.
- Institute of Archaeology CASS, Institute of Archaeology of Beijing (1984) 1981–1983 年琉璃河西周燕国墓地发掘简报 (Brief report on the excavation of the Western Zhou Yan state cemetery at Liulihe, 1981–1983). *考古 (Kaogu)* **1984**.05, 405–416+481–484+404.
- Institute of Archaeology CASS, Institute of Archaeology of Beijing (1990) 北京琉璃河1193号大墓发掘简报 (Brief report on the excavation of tomb no. 1193 in Liulihe, Beijing). *考古 (Kaogu)* **1990**.01, 20–31+97–99.
- Institute of Archaeology of Beijing (1995) 琉璃河西周燕国墓地 (1973–1977) (*Liulihe Western Zhou Yan State Cemetery, 1973–1977*). Beijing: Wenwu Press.
- Institute of Archaeology of Beijing, Department of Archaeology PKU (1996) 1995 年琉璃河周代居址发掘简报 (The 1995 season of excavation of a cemetery at the Liulihe site). *文物 (Wenwu)* **1996**.06, 16–27.
- Institute of Archaeology of Beijing, Department of Archaeology PKU, Institute of Archaeology CASS (2000) 1997 年琉璃河遗址墓葬发掘简报 (Brief report on the 1997 excavation of the Liulihe site burials). *文物 (Wenwu)* **2000**.11, 32–38.
- Johnstone-Belford E, Fallon SJ, Dipnall JF and Blau S (2022) The importance of bone sample selection when using radiocarbon analysis in cases of unidentified human remains. *Forensic Science International* **341**, 111480.
- Lee YK (2002) Building the chronology of early Chinese history. *Asian Perspectives* **41**(1), 15–42.
- Li X, Liu W, Xu Y, Dou H, Pollard AM and Liu R (2023) A view from the countryside: Radiocarbon chronology for Zaolinhetan of the pre-Zhou culture in early dynastic China. *Radiocarbon* **65**(6), 1299–1321.
- Liu K, Wu X, Guo Z, Yuan S, Ding X, Fu D and Pan Y (2021) Radiocarbon dating of oracle bones of late Shang Period in ancient China. *Radiocarbon* **63**(1), 155–175.
- Liulihe Archaeology Team (1997) 琉璃河遗址1996年度发掘简报 (Brief report on 1996 excavation of Liulihe site). *文物 (Wenwu)* **1997**.06, 4–13+11.
- Lou P (2002) 琉璃河遗址2001年度西周墓葬发掘简报 (Brief report on 2001 excavation of Western Zhou burials at Liulihe site). *北京文物与考古 (第五辑) (Beijing Cultural Relics and Archaeology)* **5**, 73–79.
- Millard AR, Annis RG, Caffell AC, Dodd LL, Fischer R, Gerrard CM, Graves CP, Hendy J, Mackenzie L, Montgomery J et al (2020) Scottish soldiers from the Battle of Dunbar 1650: A prosopographical approach to a skeletal assemblage. *PLOS ONE* **15**(12), e0243369.
- Reimer PJ, Austin WEN, Bard E, Bayliss A, Blackwell PG, Bronk Ramsey C, Butzin M, Cheng H, Edwards RL, Friedrich M et al (2020) The IntCal20 Northern Hemisphere radiocarbon age calibration curve (0–55 cal kbp). *Radiocarbon* **62**(4), 725–757.
- Shi F (2022) 2022-01-10. 琉璃河遗址两段铭文共证北京三千年建城史 (Two inscriptions at the Liulihe site testify to Beijing's 3,000-year history of city building). *人民日报海外版 (People's Daily Overseas Edition)*.
- Staff RA, Bronk Ramsey C, Bryant CL, Brock F, Payne RL, Schlolaut G, Marshall MH, Brauer A, Lamb HF, Tarasov P et al (2011) New  $^{14}\text{C}$  determinations from Lake Suigetsu, Japan: 12,000 to 0 cal bp. *Radiocarbon* **53**(3), 511–528.
- Ubelaker DH, Buchholz BA and Stewart JEB (2006) Analysis of artificial radiocarbon in different skeletal and dental tissue types to evaluate date of death. *Journal of Forensic Sciences* **51**(3), 484–488.

- Ubelaker DH, Plens CR, Soriano EP, Diniz MV, de Almeida Junior E, Junior ED, Júnior LF and Machado CEP (2022) Lag time of modern bomb-pulse radiocarbon in human bone tissues: New data from Brazil. *Forensic Science International* **331**, 111143.
- Ubelaker DH, Thomas C, Olson JE (2015) The impact of age at death on the lag time of radiocarbon values in human bone. *Forensic Science International* **251**, 56–60.
- van Klinken GJ (1999) Bone collagen quality indicators for palaeodietary and radiocarbon measurements. *Journal of Archaeological Science* **26**(6), 687–695.
- Wood R (2015) From revolution to convention: The past, present and future of radiocarbon dating. *Journal of Archaeological Science* **56**, 61–72.
- Wu Z (2012) 商周青铜器铭文暨图像集成 (Collection of inscriptions and images of bronze artifacts from the Shang and Zhou Dynasty). Shanghai: 上海古籍出版社 (*Shanghai Ancient Books Publishing House*).
- Xia-Shang-Zhou Chronology Project (2022) 夏商周断代工程报告 (The Xia-Shang-Zhou Chronology Project: Report). Beijing: 科学出版社 (*China Science Publishing*).
- Zhang X, Qiu S and Cai L (2003) 琉璃河西周墓葬的高精度年代测定 (High-precision dating of the Western Zhou tombs at Liulihe). *考古学报* (*Kaogu Xuebao*) **2003**.01, 137–160.

---

**Cite this article:** Ouyang X, Wu X, Wang J, Pan Y, Lin YH, He J, Guo J, and Cui J. A modeling radiocarbon dating for the founding of Yan Vassal State in Western Zhou Dynasty. *Radiocarbon*. <https://doi.org/10.1017/RDC.2024.117>